Proceedings of the ASME 2017 Dynamic Systems and Control Conference
DSCC2017
October 11-13, 2017, Tysons, Virginia, USA

DSCC2017-5343

PROXY-BASED OPTIMAL DYNAMIC CONTROL ALLOCATION FOR MULTI-INPUT, MULTI-OUTPUT OVER-ACTUATED SYSTEMS

Molong Duan
Department of Mechanical Engineering
University of Michigan, Ann Arbor, MI, USA
molong@umich.edu

Chinedum Okwudire
Department of Mechanical Engineering
University of Michigan, Ann Arbor, MI, USA
okwudire@umich.edu

ABSTRACT

In over-actuated systems, an output can be realized through various control effort combinations. It is desirable to allocate the control efforts dynamically (as opposed to statically) in an optimal manner. In this paper, a proxy-based control allocation approach is proposed for multi-input, multi-output over-actuated systems. Instead of using real-time optimization for control allocation, the proposed method establishes an energy optimal subspace; it then defines a causally implementable proxy to accurately measure the deviation of the controlled system from the energy optimal subspace using matrix fraction description and spectral factorization. The control allocation problem is thus converted to a regulation problem, and is solved using a standard H_∞ approach. The proposed method is validated through simulation examples, in comparison with an existing dynamic control allocation method. Significant improvements in energy efficiency without affecting the controlled output are demonstrated.

1. INTRODUCTION

Over-actuated systems are characterized by the use of more actuators compared to the degrees of freedom to be controlled [1]. This redundant actuation structure has potential to enhance accuracy, work range, fault tolerance, etc., and thus is adopted by various applications [2–9]. For example, redundant thrusters are employed in spacecraft to preserve maneuverability in the event of thruster failure [4]. In servo systems, over-actuation is used to improve motion range [2], accuracy [7] and energy efficiency [8,10]. Over-actuation also provides a promising solution to structural flexibility issues in lightweight motion systems [3].

A major focus in controlling over-actuated systems is the distribution of control efforts among the redundant actuators. Due to redundancy, a desired output performance can be realized through various distributions of redundant control inputs, thus additional criteria are required to determine the optimal distribution. This distribution process is referred to as control (effort) allocation [11], and the minimization of the 2-norm (or energy) of the control inputs is commonly selected as optimal allocation criterion [5,6,11–17]. Control allocation is usually employed in a two-stage framework, in which a high level nominal controller (also referred as 'virtual controller') [5,11–13] determines the non-redundant overall control efforts needed to realize the output; while a dedicated allocator distributes the control efforts to redundant input channels according to the specified additional criteria [11–15].

Control allocation methods are extensively developed for systems with strong input redundancy, where there exists a set of control inputs that do not affect system internal states [12–15]. Under this condition, the 2-norm-minimizing control allocation is a quadratic programming problem, to which various numerical methods (e.g., redistributed pseudoinverse, fixed-point methods) can be applied [14]. However, strong input redundancy conditions are restrictive since they require exact collocation of actuators or truncation of high order dynamics. In practical applications, discarding these dynamics may affect the control output (performance) and even lead to instability [13].

To facilitate control allocation considering high order dynamics, weak input redundancy is defined as an extension to strong input redundancy [16], where the internal states are no longer required to be invariant [16–18]. However, weak input redundant systems are by nature more challenging since optimal dynamic allocation (as opposed to static allocation) needs to be considered. General control allocation problems for weakly input redundant systems can be solved within the model predictive control framework [17], where the computational intensive real-time optimization may be restrictive for certain applications. Galeani et al. [18] explored static state feedback

structures for optimal control allocation using regulator theory, and a finite dimension relaxation was employed to reduce the computational cost. However, this relaxation leads to a hybrid system, and the associated switching events may introduce undesirable transients. Zaccarian [16] proposed a dynamic allocation method based on a static redundancy model in weakly input redundant systems. While this approach [16] greatly simplifies the problem and reduces computational burden, it is incapable of optimally allocating dynamic control efforts (e.g., control efforts with non-zero frequency content). Moreover, the approaches in [16] and [18] both do not guarantee invariance of the controlled output (i.e., control performance) during control allocation.

The present authors explored the dual-input, single-output (DISO) weakly input redundant systems, and showed that the energy optimal inputs satisfy an dynamic optimal control ratio [19,20]. The optimal control ratio is shown to be non-causal and causal approximation is employed for practical applications on a hybrid feed drive [19–21]. To address the energy efficiency loss due to approximation, a proxy-based method is proposed in [22], where the non-causal ratio is converted to a causal stable proxy, which measures the energy efficiency in real time and can be regulated to approach energy optimality. Building on [22], the proxy-based method for DISO system is extended to multi-input, multi-output (MIMO) systems through matrix fraction description and spectral factorization in this paper. The rest of this paper is organized as follows: In Section 2, a brief background on optimal control ratio and proxy-based control allocation for DISO systems is provided. In Section 3, the optimal control subspace, a multivariable proxy and its application in control allocation is discussed. The proposed proxy-based control allocation is compared in simulations with an existing dynamic control allocation method in Section 4, followed by conclusions and future work in Section 5.

2. BACKGROUND ON PROXY-BASED CONTROL ALLOCATION FOR DISO SYSTEMS

Consider a linear time-invariant (LTI) DISO system $\mathbf{G} = [G_1, G_2]$, with two inputs $\mathbf{u} = [u_1, u_2]^{\mathrm{T}}$, a single output y and disturbance $\mathbf{d}$ (shown in Fig. 1), i.e.

$$y = \begin{bmatrix} G_1 & G_2 \end{bmatrix} \begin{bmatrix} u_1 & u_2 \end{bmatrix}^{\mathrm{T}} + \mathbf{G}_{\mathrm{d}}\mathbf{d} \tag{1}$$

(Here disturbance $\mathbf{d}$ represents general external inputs such as a reference signal, noise, etc.) This system has more inputs than outputs, and is defined as weakly input redundant [16] as

$$\mathrm{Ker}\left(\mathbf{G}(s)\right) \neq \varnothing \tag{2}$$

for almost all s, where Ker yields the kernel (null space) of the corresponding matrices. In weakly input redundant systems, there exists a family of input trajectories that yield the same output trajectory due to redundancy [16,17]. Assume a nominal control input $\mathbf{u}_0$ which yields a desirable output y_0 under disturbance $\mathbf{d}_0$, i.e.,

$$\mathbf{G}\mathbf{u}_0 = y_0 - \mathbf{G}_{\mathrm{d}}\mathbf{d}_0 \tag{3}$$

The family of control signals which replicate y_0 under $\mathbf{d}_0$ formulates a set Ω, given by

$$\Omega(\mathbf{u}_0) \triangleq \left\{ \mathbf{u} \in \mathbb{R}^2 : \mathbf{G}(\mathbf{u}_0 - \mathbf{u}) = 0 \right\} \tag{4}$$

As shown in Fig. 1, the goal of energy optimal control allocation is to formulate a mapping $\mathbf{P}$ between $\mathbf{u}_0$ and $\mathbf{u} \in \Omega$ such that control energy is minimized without altering $y = y_0$.

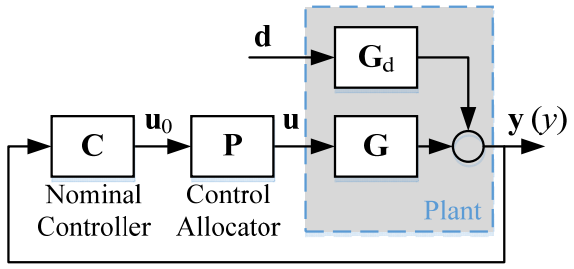

FIGURE 1: GENERALIZED BLOCK DIAGRAM FOR CONTROL ALLOCATION

Define a typical quadratic energy cost

$$J(\mathbf{u}) \triangleq \int \left(\mathbf{u}^{\mathrm{T}} \mathbf{R} \mathbf{u} \right) dt = \int \begin{bmatrix} u_1 \\ u_2 \end{bmatrix}^{\mathrm{T}} \begin{bmatrix} R_{11} & R_{12} \\ R_{12} & R_{22} \end{bmatrix} \begin{bmatrix} u_1 \\ u_2 \end{bmatrix} dt \tag{5}$$

with a positive definite square symmetric $\mathbf{R}$, and define set Ω as the optimization space. The energy optimal control signal's variation should satisfy

$$\delta J = 0 \Rightarrow \int \left(\delta \mathbf{u}^{\mathrm{T}} \mathbf{R} \mathbf{u} \right) dt = 0 \tag{6}$$

Also, the variation should satisfy

$$G_1 \delta u_1 + G_2 \delta u_2 = 0 \tag{7}$$

to ensure $\mathbf{u}$ remains in Ω defined in Eq. (4). Combining Eqs. (6) and (7), and applying the fundamental lemma of calculus of variations [23], the optimal control inputs (marked with $\hat{}$) satisfy an optimal ratio [19,20,22] defined as

$$\beta^* \triangleq \frac{\hat{u}_1}{\hat{u}_2} = \frac{R_{22} G_1^* - R_{12} G_2^*}{R_{11} G_2^* - R_{12} G_1^*} \tag{8}$$

where the superscript * represents the adjoint operator [24], which leads to a non-causal relationship between the control inputs that minimize J. In order to causally evaluate the deviation from this control ratio, a proxy-based allocation method is proposed in [22], where proxy u_{D} is defined as

$$\begin{aligned} u_{\mathrm{D}} &= \beta_2 u_1 - \beta_1 u_2 \\ \beta_1 &\triangleq \frac{R_{22} G_{1\mathrm{n}}^* - R_{12} G_{2\mathrm{n}}^*}{\psi};\ \beta_2 \triangleq \frac{R_{11} G_{2\mathrm{n}}^* - R_{12} G_{1\mathrm{n}}^*}{\psi} \end{aligned} \tag{9}$$

where G_{1n} and G_{2n} are respectively the numerators of the original transfer functions G_1 and G_2, ψ is a user-defined denominator to ensure properness, and β_1 and β_2 formulate a factorization of β^*. The adjoint operation of numerators can be causally implemented and thus u_D can be evaluated in real time. Accordingly, the control allocation problem is converted to a regulation problem on proxy u_D, which can be realized using various traditional single-input, single-output control design methods. However, the proxy-based allocation framework proposed in [22] is only applicable to DISO systems; the rest of this paper extends it to MIMO systems.

3. PROXY-BASED ENERGY OPTIMAL CONTROL ALLOCATION FOR MIMO SYSTEMS

3.1. ENERGY OPTIMAL SUBSPACE

Consider a general MIMO weakly input redundant system given by

$$\mathbf{y} = \mathbf{G}\mathbf{u} + \mathbf{G}_d\mathbf{d} \tag{10}$$

where $\mathbf{y} \in \mathbb{R}^{n_y}$ is the output of the system, while $\mathbf{u} \in \mathbb{R}^{n_u}$, $\mathbf{d} \in \mathbb{R}^{n_d}$ are the control input and disturbance, respectively. Weak input redundancy requires $n_u > n_y$, and

$$n_r = n_u - n_y \tag{11}$$

is defined as the redundancy degree. Without loss of generality, the first n_y control inputs are assumed to formulate a non-redundant control input set, i.e. the overall system transfer function matrix is divided as

$$\mathbf{G} = \begin{bmatrix} \mathbf{G}_p & \mathbf{G}_r \end{bmatrix}; \mathbf{u} = \begin{bmatrix} \mathbf{u}_p^T & \mathbf{u}_r^T \end{bmatrix}^T \tag{12}$$

where $\mathbf{G}_p$ is a nonsingular square transfer function matrix from the first n_y principal control inputs $\mathbf{u}_p$ to the outputs, and $\mathbf{G}_r$ ($n_y \times n_r$) is a transfer function matrix from the remaining n_r redundant control inputs $\mathbf{u}_r$ to the outputs. Due to the nature of over-actuated systems, there exists null space within which the control inputs' variations would not affect the system outputs, i.e.

$$\begin{bmatrix} \mathbf{G}_p & \mathbf{G}_r \end{bmatrix} \begin{bmatrix} \delta\mathbf{u}_p \\ \delta\mathbf{u}_r \end{bmatrix} = \mathbf{0} \Rightarrow \delta\mathbf{u}_p = -\mathbf{G}_p^{-1}\mathbf{G}_r\delta\mathbf{u}_r \tag{13}$$

Same as in the DISO systems, a quadratic cost is defined for the MIMO system as

$$J(\mathbf{u}) = \int \mathbf{u}^T\mathbf{R}\mathbf{u}dt = \int \begin{bmatrix} \mathbf{u}_p \\ \mathbf{u}_r \end{bmatrix}^T \begin{bmatrix} \mathbf{R}_p & \mathbf{R}_{pr} \\ \mathbf{R}_{pr}^T & \mathbf{R}_r \end{bmatrix} \begin{bmatrix} \mathbf{u}_p \\ \mathbf{u}_r \end{bmatrix} dt \tag{14}$$

where $\mathbf{R}$ is a positive definite symmetric matrix divided according to the first n_y principal control inputs and n_r redundant inputs. To achieve energy optimality, the variation of J should satisfy

$$\delta J = \int \begin{bmatrix} \delta\mathbf{u}_p \\ \delta\mathbf{u}_r \end{bmatrix}^T \begin{bmatrix} \mathbf{R}_p & \mathbf{R}_{pr} \\ \mathbf{R}_{pr}^T & \mathbf{R}_r \end{bmatrix} \begin{bmatrix} \mathbf{u}_p \\ \mathbf{u}_r \end{bmatrix} dt = 0 \tag{15}$$

Consider the variation within the null space specified by Eq. (13)

$$\begin{aligned} &\int \left(-\mathbf{G}_p^{-1}\mathbf{G}_r\delta\mathbf{u}_r\right)^T \mathbf{R}_p\mathbf{u}_p + \left(-\mathbf{G}_p^{-1}\mathbf{G}_r\delta\mathbf{u}_r\right)^T \mathbf{R}_{pr}\mathbf{u}_r \\ &+\delta\mathbf{u}_r^T\mathbf{R}_{pr}^T\mathbf{u}_p + \delta\mathbf{u}_r^T\mathbf{R}_r\mathbf{u}_r dt = 0 \end{aligned} \tag{16}$$

Taking the adjoint operation of transfer function matrix $\mathbf{G}_p^{-1}\mathbf{G}_r$

$$\begin{aligned} \int \delta\mathbf{u}_r^T \{&[(\mathbf{G}_p^{-1}\mathbf{G}_r)^*\mathbf{R}_p - \mathbf{R}_{pr}^T]\mathbf{u}_p \\ &+[(\mathbf{G}_p^{-1}\mathbf{G}_r)^*\mathbf{R}_{pr} - \mathbf{R}_r]\mathbf{u}_r\} dt = 0 \end{aligned} \tag{17}$$

The following condition holds for the energy optimal control inputs based on the fundamental lemma of calculus of variation applied to multivariable vectors [23].

$$\left[\left(\mathbf{G}_p^{-1}\mathbf{G}_r\right)^*\mathbf{R}_p - \mathbf{R}_{pr}^T\right]\mathbf{u}_p = \left[\mathbf{R}_r - \left(\mathbf{G}_p^{-1}\mathbf{G}_r\right)^*\mathbf{R}_{pr}\right]\mathbf{u}_r \tag{18}$$

Note that $(\mathbf{G}_p^{-1}\mathbf{G}_r)^*$ is non-causal (because of the adjoint operator), and the relation in Eq. (18) formulates an optimal control subspace, which is a natural extension of the concept of the optimal control ratio in Eq. (8).

3.2. PROXY AS MEASUREMENT OF DEVIATION FROM THE OPTIMAL CONTROL SUBSPACE

In order to establish a causal stable deviation measurement (proxy) from the optimal subspace specified by Eq. (18), a decomposition similar to that for DISO systems in Eq. (9) is needed. However unlike in Eq. (9) where the scalar transfer function's numerators and denominator can be directly extracted, $\mathbf{G}_p^{-1}\mathbf{G}_r$ is a transfer function matrix and thus matrix fraction description [25] is used. Here $\mathbf{G}_p^{-1}\mathbf{G}_r$ is written as

$$\mathbf{G}_p^{-1}(s)\mathbf{G}_r(s) = \mathbf{N}(s)\mathbf{D}^{-1}(s) \tag{19}$$

where $\mathbf{N}$ ($n_y \times n_r$) and $\mathbf{D}$ ($n_r \times n_r$) are coprime transfer function polynomials without denominators, such that Eq. (19) formulates a right coprime fraction of $\mathbf{G}_p^{-1}\mathbf{G}_r$. Note that here $\mathbf{N}$ and $\mathbf{D}$ are not unique: all possible coprime $\mathbf{N}$ and $\mathbf{D}$ pairs are related to each other through unimodular transformation matrices [25]. The importance of this right coprime fraction is that $\mathbf{N}$ and $\mathbf{D}$ only contain the numerator polynomials, whose adjoint

$$\left(\mathbf{N}(s)\right)^* = \mathbf{N}^T(-s);\ \left(\mathbf{D}(s)\right)^* = \mathbf{D}^T(-s) \tag{20}$$

are also numerator polynomials due to $s^* = -s$ [26], which does not lead to instability. Deviation from Eq. (18), which originally cannot be causally evaluated, is measured by proxy $\mathbf{u}_D$ defined as

$$\mathbf{u}_D = \boldsymbol{\beta}_p\mathbf{u}_p - \boldsymbol{\beta}_r\mathbf{u}_r \tag{21}$$

where

$$\begin{aligned}\boldsymbol{\beta}_{\mathrm{p}} &= \boldsymbol{\psi}^{-1}\left(\mathbf{N}^{*}\mathbf{R}_{\mathrm{p}} - \mathbf{D}^{*}\mathbf{R}_{\mathrm{pr}}^{\mathrm{T}}\right)\\ \boldsymbol{\beta}_{\mathrm{r}} &= \boldsymbol{\psi}^{-1}\left(\mathbf{D}^{*}\mathbf{R}_{\mathrm{r}} - \mathbf{N}^{*}\mathbf{R}_{\mathrm{pr}}\right)\end{aligned} \tag{22}$$

Here $\boldsymbol{\psi}$ is defined as a square ($n_{\mathrm{r}} \times n_{\mathrm{r}}$) nonsingular numerator polynomial with minimum phase zeros such that both $\boldsymbol{\psi}^{-1}\mathbf{D}^{*}$ and $\boldsymbol{\psi}^{-1}\mathbf{N}^{*}$ are proper and stable transfer function matrices, and can thus be evaluated in real time.

It is clear from Eqs. (18) and (21) that enforcing $\mathbf{u}_{\mathrm{D}} = \mathbf{0}$ ensures energy optimality. However this perfect condition may not be always satisfied due to various reasons such as limited control bandwidth, non-minimum phase (NMP) zeros, etc. [22]. Therefore, it is instrumental to understand how nonzero $\mathbf{u}_{\mathrm{D}}$ is related to the energy cost J. For any control signal $\mathbf{u} = \hat{\mathbf{u}} + \delta\mathbf{u}$ which belongs to $\Omega(\hat{\mathbf{u}})$, its energy cost J is decomposed into

$$J(\mathbf{u}) = \underbrace{\int \hat{\mathbf{u}}^{\mathrm{T}}\mathbf{R}\hat{\mathbf{u}}dt}_{J(\hat{\mathbf{u}})} + \underbrace{2\int \delta\mathbf{u}^{\mathrm{T}}\mathbf{R}\hat{\mathbf{u}}dt}_{J_{\mathrm{cc}}} + \underbrace{\int \delta\mathbf{u}^{\mathrm{T}}\mathbf{R}\delta\mathbf{u}dt}_{J(\delta\mathbf{u})} \tag{23}$$

where $J(\hat{\mathbf{u}})$ and $J(\delta\mathbf{u})$ are positive definite terms representing the optimal energy cost and energy cost of $\delta\mathbf{u}$. Note that $\delta\mathbf{u}$ is assumed to satisfy the null space condition specified by Eq. (13), such that the cross coupling term $J_{\mathrm{cc}} = 0$, i.e.

$$\begin{aligned}J_{\mathrm{cc}} &= 2\int \begin{bmatrix}\delta\mathbf{u}_{\mathrm{p}}\\ \delta\mathbf{u}_{\mathrm{r}}\end{bmatrix}^{\mathrm{T}}\begin{bmatrix}\mathbf{R}_{\mathrm{p}} & \mathbf{R}_{\mathrm{pr}}\\ \mathbf{R}_{\mathrm{pr}}^{\mathrm{T}} & \mathbf{R}_{\mathrm{r}}\end{bmatrix}\begin{bmatrix}\hat{\mathbf{u}}_{\mathrm{p}}\\ \hat{\mathbf{u}}_{\mathrm{r}}\end{bmatrix}dt\\ &= 2\int \delta\mathbf{u}_{\mathrm{p}}^{\mathrm{T}}\mathbf{R}_{\mathrm{p}}\hat{\mathbf{u}}_{\mathrm{p}} + \delta\mathbf{u}_{\mathrm{p}}^{\mathrm{T}}\mathbf{R}_{\mathrm{pr}}\hat{\mathbf{u}}_{\mathrm{r}} + \delta\mathbf{u}_{\mathrm{r}}^{\mathrm{T}}\mathbf{R}_{\mathrm{pr}}^{\mathrm{T}}\hat{\mathbf{u}}_{\mathrm{p}} + \delta\mathbf{u}_{\mathrm{r}}^{\mathrm{T}}\mathbf{R}_{\mathrm{r}}\hat{\mathbf{u}}_{\mathrm{r}}dt\\ &= 2\int \delta\mathbf{u}_{\mathrm{r}}^{\mathrm{T}}\{[(\mathbf{G}_{\mathrm{p}}^{-1}\mathbf{G}_{\mathrm{r}})^{*}\mathbf{R}_{\mathrm{p}} - \mathbf{R}_{\mathrm{pr}}^{\mathrm{T}}]\hat{\mathbf{u}}_{\mathrm{p}}\\ &\qquad + [(\mathbf{G}_{\mathrm{p}}^{-1}\mathbf{G}_{\mathrm{r}})^{*}\mathbf{R}_{\mathrm{pr}} - \mathbf{R}_{\mathrm{r}}]\hat{\mathbf{u}}_{\mathrm{r}}\}dt = 0\end{aligned} \tag{24}$$

This zero cross coupling term indicates that the $J(\delta\mathbf{u})$ comprises the positive definite energy increment $J(\mathbf{u}) = J(\hat{\mathbf{u}}) + J(\delta\mathbf{u})$ from the optimal control inputs. Knowing that $\mathbf{u}_{\mathrm{D}} = \mathbf{0}$ when $\mathbf{u} = \hat{\mathbf{u}}$, Eq. (21) can be re-written as

$$\mathbf{u}_{\mathrm{D}} = \boldsymbol{\beta}_{\mathrm{p}}\delta\mathbf{u}_{\mathrm{p}} - \boldsymbol{\beta}_{\mathrm{r}}\delta\mathbf{u}_{\mathrm{r}} \tag{25}$$

Combined with Eq. (13), $\delta\mathbf{u}$ is related to the proxy $\mathbf{u}_{\mathrm{D}}$ as

$$\begin{aligned}\delta\mathbf{u}_{\mathrm{r}} &= -\left[\boldsymbol{\beta}_{\mathrm{p}}\left(\mathbf{G}_{\mathrm{p}}^{-1}\mathbf{G}_{\mathrm{r}}\right) + \boldsymbol{\beta}_{\mathrm{r}}\right]^{-1}\mathbf{u}_{\mathrm{D}} = -\mathbf{D}\boldsymbol{\Pi}^{-1}\boldsymbol{\psi}\mathbf{u}_{\mathrm{D}}\\ \delta\mathbf{u}_{\mathrm{p}} &= \mathbf{G}_{\mathrm{p}}^{-1}\mathbf{G}_{\mathrm{r}}\left[\boldsymbol{\beta}_{\mathrm{p}}\left(\mathbf{G}_{\mathrm{p}}^{-1}\mathbf{G}_{\mathrm{r}}\right) + \boldsymbol{\beta}_{\mathrm{r}}\right]^{-1}\mathbf{u}_{\mathrm{D}} = \mathbf{N}\boldsymbol{\Pi}^{-1}\boldsymbol{\psi}\mathbf{u}_{\mathrm{D}}\end{aligned} \tag{26}$$

where $\boldsymbol{\Pi}$ is defined to be a self-adjoint system given by

$$\boldsymbol{\Pi} = \begin{bmatrix}\mathbf{N}\\ -\mathbf{D}\end{bmatrix}^{*}\mathbf{R}\begin{bmatrix}\mathbf{N}\\ -\mathbf{D}\end{bmatrix} \tag{27}$$

and according to Eq. (22),

$$\boldsymbol{\beta}_{\mathrm{p}}\left(\mathbf{G}_{\mathrm{p}}^{-1}\mathbf{G}_{\mathrm{r}}\right) + \boldsymbol{\beta}_{\mathrm{r}} = \boldsymbol{\psi}^{-1}\boldsymbol{\Pi}\mathbf{D}^{-1} \tag{28}$$

Applying Parseval's theorem and the frequency domain expression from Eq. (26) to (28), the energy increment due to deviation from optimal subspace $\delta J = J(\mathbf{u}) - J(\hat{\mathbf{u}}) = J(\delta\mathbf{u})$ is given by

$$\begin{aligned}\delta J &= \int \delta\mathbf{u}^{\mathrm{T}}\mathbf{R}\delta\mathbf{u}dt = \frac{1}{2\pi}\int \delta\mathbf{u}^{*}(\omega)\mathbf{R}\delta\mathbf{u}(\omega)\\ &= \frac{1}{2\pi}\int \mathbf{u}_{\mathrm{D}}^{*}\boldsymbol{\psi}^{*}\left(\boldsymbol{\Pi}^{-1}\right)^{*}\underbrace{\begin{bmatrix}\mathbf{N}\\ -\mathbf{D}\end{bmatrix}^{*}\mathbf{R}\begin{bmatrix}\mathbf{N}\\ -\mathbf{D}\end{bmatrix}}_{=\boldsymbol{\Pi}}\boldsymbol{\Pi}^{-1}\boldsymbol{\psi}\mathbf{u}_{\mathrm{D}}d\omega\\ &= \frac{1}{2\pi}\int \mathbf{u}_{\mathrm{D}}^{*}\boldsymbol{\psi}^{*}\left(\boldsymbol{\Pi}^{-1}\right)^{*}\boldsymbol{\psi}\mathbf{u}_{\mathrm{D}}d\omega\end{aligned} \tag{29}$$

The energy increment δJ would be the square of the two norm of the proxy $\mathbf{u}_{\mathrm{D}}$, i.e.

$$\delta J = \left\|\mathbf{u}_{\mathrm{D}}\right\|_{2}^{2} \tag{30}$$

given

$$\boldsymbol{\Pi} = \boldsymbol{\psi}\boldsymbol{\psi}^{*} \tag{31}$$

The implication of Eq. (30) is that the deviation of $\mathbf{u}_{\mathrm{D}}$ from zero is directly proportional to the deviation of $J(\mathbf{u})$ from its optimal value of $J(\hat{\mathbf{u}})$. Accordingly, decreasing the 2-norm of $\mathbf{u}_{\mathrm{D}}$ via regulation of the proxy $\mathbf{u}_{\mathrm{D}}$ strictly enhances the energy efficiency.

Notice from Eq. (27) that the self-adjoint $\boldsymbol{\Pi}$ consists only of zeros symmetrically placed about the imaginary axis. One can therefore collect all the minimum phase zeros of $\boldsymbol{\Pi}$ into a stable and causally implementable $\boldsymbol{\psi}$; this decomposition in Eq. (31) is referred as left spectral factorization [27]. Note that $\mathbf{N}$ and $\mathbf{D}$ are coprime (share no common zeros) and $\mathbf{R}$ is positive definite, indicating $\boldsymbol{\Pi}$ has no zeros on the imaginary axis because

$$\boldsymbol{\Pi}(j\omega) = \begin{bmatrix}\mathbf{N}(-j\omega)\\ -\mathbf{D}(-j\omega)\end{bmatrix}^{\mathrm{T}}\mathbf{R}\begin{bmatrix}\mathbf{N}(j\omega)\\ -\mathbf{D}(j\omega)\end{bmatrix} > 0 \tag{32}$$

holds for all $s = j\omega$. Under this condition, stable and minimum phase solutions $\boldsymbol{\psi}$ to Eq. (31) always exist [27].

3.3. PROXY-BASED ALLOCATOR DESIGN

As Fig. 1 illustrates, the control allocator $\mathbf{P}$ aims at redistributing control efforts $\mathbf{u}_0$ within $\Omega(\mathbf{u}_0)$ such that the control performance is preserved. Therefore, according to Eq. (13), (as shown in Fig. 2) it is assumed that:

$$\mathbf{u} = \mathbf{u}_0 + \begin{bmatrix}-\mathbf{N}\boldsymbol{\psi}_0^{-1}\\ \mathbf{D}\boldsymbol{\psi}_0^{-1}\end{bmatrix}\mathbf{v} \tag{33}$$

where $\mathbf{v} \in \mathbb{R}^{n_{\mathrm{r}}}$ is an arbitrary signal while $\boldsymbol{\psi}_0$ is a user defined nonsingular square polynomial transfer function numerator matrix with minimum phase zeros; $\boldsymbol{\psi}_0$ is a pre-filter that helps to eliminate undesirable pole dynamics in the original system. Note that Eq. (33) satisfies the null space defined in Eq. (13) as

$$\begin{bmatrix}\mathbf{G}_p & \mathbf{G}_r\end{bmatrix}\begin{bmatrix}-\mathbf{N}\boldsymbol{\psi}_0^{-1}\\ \mathbf{D}\boldsymbol{\psi}_0^{-1}\end{bmatrix}\mathbf{v}=\mathbf{0} \tag{34}$$

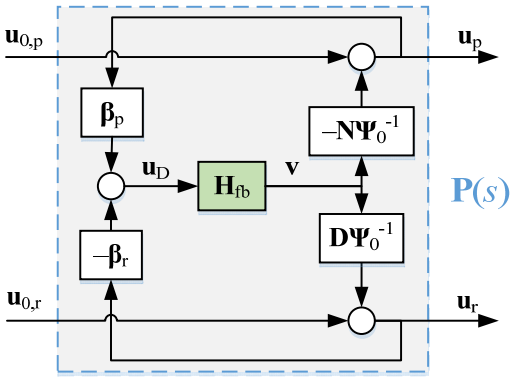

FIGURE 2: PROPROSED CONTROL ALLOCATOR

Assume the proxy of the nominal controller $\mathbf{u}_0$ (before allocation) is defined as

$$\mathbf{u}_{D0}=\begin{bmatrix}\boldsymbol{\beta}_p & -\boldsymbol{\beta}_r\end{bmatrix}\mathbf{u}_0 \tag{35}$$

Then the proxy after allocation $\mathbf{u}_D$ is given by

$$\mathbf{u}_D=\mathbf{u}_{D0}+\Delta\mathbf{u}_D=\mathbf{u}_{D0}+\underbrace{\begin{bmatrix}\boldsymbol{\beta}_p & -\boldsymbol{\beta}_r\end{bmatrix}\begin{bmatrix}-\mathbf{N}\boldsymbol{\psi}_0^{-1}\\ \mathbf{D}\boldsymbol{\psi}_0^{-1}\end{bmatrix}}_{\triangleq\mathbf{H}_v}\mathbf{v} \tag{36}$$

where $\mathbf{H}_v$ is a square ($n_r \times n_r$) dynamic system, mapping $\mathbf{v}$ to its manipulation of the proxy $\Delta\mathbf{u}_D$. Notice from Eq. (36) that one possibility is to make $\mathbf{u}_D = \mathbf{0}$ via feedforward control using $\mathbf{v} = -\mathbf{H}_v^{-1}\mathbf{u}_{D0}$, which ideally would yield the energy optimal control input. However, such a feedforward design is not robust and is limited by possible NMP zeros within $\mathbf{H}_v$ [21]. Therefore a feedback relationship

$$\mathbf{v}=\mathbf{H}_{fb}\mathbf{u}_D \tag{37}$$

is assumed as shown in Fig. 2. With this assumption, $\mathbf{H}_{fb}$ can be designed using various MIMO controller synthesis methods. Here a representative H_∞ controller synthesis framework [28] is illustrated in Fig. 3, since infinity system norm marks the upper bound on the signal 2-norm gain. In Fig. 3, $\mathbf{W}_d$ is a weighting filter describing the disturbance profile; $\mathbf{v}_w$ is signal $\mathbf{v}$ filtered by $\mathbf{W}_v$ to penalize the high frequency component; $\mathbf{U}_{0,d}$ represents the transfer function matrix from disturbance to the nominal control $\mathbf{u}_0$ given by

$$\mathbf{U}_{0,d}=\left(\mathbf{I}-\mathbf{CG}\right)^{-1}\mathbf{CG}_d \tag{38}$$

Note that $\mathbf{U}_{0,d}$ is invariant with respect to both $\mathbf{P}$ and $\mathbf{H}_{fb}$, since the allocation process works in the null space and output is invariant. The equivalent plant marked in the blue box in Fig. 3 is referred to as $\mathbf{L}$, i.e.

$$\begin{bmatrix}\mathbf{v}_w\\ \mathbf{u}_D\end{bmatrix}=\mathbf{Ld} \tag{39}$$

Through feedback $\mathbf{H}_{fb}$, the infinity norm of $\mathbf{L}$ is minimized with standard H_∞ solvers. In cases where the allocator is expected to be designed without knowledge of the nominal controller $\mathbf{C}$, the frequency profile of $\mathbf{u}_{D0}$ can be assumed to be correlated with the disturbance frequency profile, i.e. the two blocks with dashed lines in Fig. 3 are omitted and the sizes of $\mathbf{W}_d$ and $\mathbf{d}$ are adjusted to conform to the dimension of $\mathbf{u}_{D0}$.

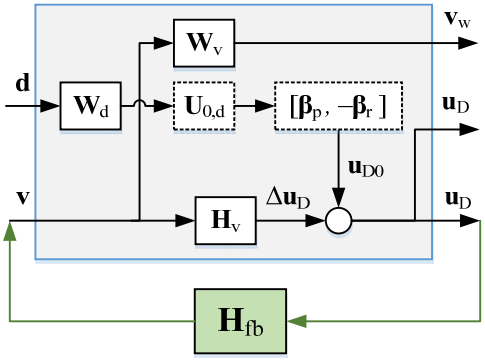

FIGURE 3: H_∞ CONTROLLER SYNTHESIS OF CONTROL ALLOCATOR

4. SIMULATION EXAMPLES

Simulation examples from [16] are used to illustrate the proposed proxy-based control allocation method. System $\mathbf{G}$ is defined to be a 3-input, 1-output system with state space realization

$$\left[\begin{array}{c|cc}A & B\\ \hline C & D\end{array}\right]=\left[\begin{array}{cc|ccc}-0.157 & -0.094 & 0.87 & 0.253 & 0.743\\ -0.416 & -0.45 & 0.39 & 0.354 & 0.65\\ \hline 0 & 1 & 0 & 0 & 0\end{array}\right] \tag{40}$$

As expressed in Eqs. (10) and (12), the first $n_y = 1$ input channel formulates a non-redundant set and the transfer function matrix is divided as

$$\mathbf{G}=\begin{bmatrix}\mathbf{G}_p & \mathbf{G}_r\end{bmatrix}=\frac{\begin{bmatrix}0.39(s-0.77)\\ 0.354(s-0.1403)\\ 0.65(s-0.3185)\end{bmatrix}^T}{s^2+0.607s+0.1098} \tag{41}$$

Note that the system $\mathbf{G}$ is a stable system with NMP zeros in each control channel. With this matrix partition, $\mathbf{G}_p^{-1}\mathbf{G}_r$ is achieved and corresponding right coprime matrix fraction ($\mathbf{N}$ and $\mathbf{D}$) defined in Eq. (19) is calculated as

$$\mathbf{G}_p^{-1}\mathbf{G}_r = \begin{bmatrix} \dfrac{0.90769(s-0.1403)}{s-0.77} & \dfrac{1.6667(s-0.3185)}{s-0.77} \end{bmatrix}$$
$$= \underbrace{\begin{bmatrix} 0.4793 & 0.90769(s-0.1403) \end{bmatrix}}_{\mathbf{N}} \underbrace{\begin{bmatrix} -1.3173 & s-0.77 \\ 1 & 0 \end{bmatrix}^{-1}}_{\mathbf{D}} \quad (42)$$

With same $\mathbf{R}$ = diag(100,1,1) defined in [16], the self-adjoint system is given by

$$\mathbf{\Pi} = \begin{bmatrix} \mathbf{N} \\ -\mathbf{D} \end{bmatrix}^{*} \mathbf{R} \begin{bmatrix} \mathbf{N} \\ -\mathbf{D} \end{bmatrix} = \begin{bmatrix} 24.913 & 41.429(s-0.1203) \\ -41.429(s+0.1203) & -83.39(s+0.163)(s-0.163) \end{bmatrix} \quad (43)$$

and its spectral factorization is calculated as

$$\mathbf{\psi} = \begin{bmatrix} 4.9913 & 0 \\ -8.3002(s+0.1203) & 3.8075(s+0.2901) \end{bmatrix} \quad (44)$$

Note that although the original system $\mathbf{G}$ contains NMP zeros, $\mathbf{\Pi}$ is always self-adjoint and a minimum phase spectral factor $\mathbf{\psi}$ can always be found to satisfy Eq. (31). Accordingly, $\boldsymbol{\beta}_p$ and $\boldsymbol{\beta}_r$ defined in Eq. (22) are given by

$$\boldsymbol{\beta}_p = \begin{bmatrix} 9.4351 & -\dfrac{3.272s+0.8715}{s+0.2901} \end{bmatrix}^{T}$$
$$\boldsymbol{\beta}_r = \begin{bmatrix} -0.2639 & 0.2 \\ -\dfrac{0.838s+0.2717}{s+0.2901} & \dfrac{0.4368s+0.05252}{s+0.2901} \end{bmatrix} \quad (45)$$

which is causal and stable, thus $\mathbf{u}_D$ is evaluated and regulated in real time.

The same LQG controller as in [16] is used as the nominal controller $\mathbf{C}$. Without loss of generality, disturbance $\mathbf{d}$ defined in Fig. 1 is assumed to be affecting output from the first control channel, i.e. $\mathbf{G}_d = \mathbf{G}(:,1)$. Here two nominal disturbance profiles are considered:

(a) Step disturbance: $\mathbf{d} = 1$ ($t > 0$);

(b) Sinusoidal disturbance at 1 Hz: $\mathbf{d} = 100\sin(2\pi t)$;

Accordingly, $\mathbf{W}_d$ is defined as an integrator with resonance term

$$\mathbf{W}_d(s) \triangleq \frac{1}{s+\varepsilon} \frac{\omega_0^2}{s^2+2\zeta\omega_0 s+\omega_0^2} \quad (46)$$

where $\omega_0 = 2\pi$ rad/s (i.e. 1Hz), $\zeta = 0.1$ and $\varepsilon = 10^{-5}$ rad/s are used. In other words, the internal model principle [29] is employed in $\mathbf{W}_d$ to magnify the targeted frequency ranges. Weighting filter $\mathbf{W}_v$ in Fig. 2 is defined as a high pass filter:

$$\mathbf{W}_v(s) \triangleq \frac{\omega_2}{\omega_1} \frac{s+\omega_1}{s+\omega_2} \quad (47)$$

where $\omega_1 = 100\pi$ rad/s (i.e. 50 Hz) and $\omega_2 = 1000\pi$ rad/s (i.e. 500 Hz). In the same vein, $\mathbf{\psi}_0^{-1}$ in the allocator structure (Fig. 3) is designed to be a diagonal transfer function consisting of identical third order low pass Butterworth filters each with a 10 Hz cutoff frequency. The designs of both $\mathbf{W}_v$ and $\mathbf{\psi}_0$ ensure that only the low frequency contents of the control efforts are redistributed within the allocator. This arises from practical robustness concerns as the model tends to be less accurate at higher frequencies.

Following the H_∞ design framework introduced in Fig. 3, $\mathbf{H}_{fb}$ is designed without considering the controller dynamics, such that $\mathbf{L}$ maps the input $\mathbf{u}_{D0}$ to the output $[\mathbf{v}_w^T, \mathbf{u}_D^T]^T$. This synthesis calculation is conducted with MATLAB 8® H_∞ synthesis tool. The open loop (OL) and closed loop (CL) Bode plots of $\mathbf{L}$ are illustrated in Fig. 4. Note that, in open loop, input $\mathbf{u}_{D0}$ does not affect $\mathbf{v}_w$, and it only diagonally contributes to the proxy $\mathbf{u}_D$. These diagonal components are inherited from $\mathbf{W}_d$ defined in Eq. (46), and are the major contributors to $\mathbf{L}$ in open loop. The large open loop DC gains of $\mathbf{L}$ are flattened and the resonance is smoothed with closed loop feedback $\mathbf{H}_{fb}$, indicating that the low frequency components as well as the resonant peak in $\mathbf{u}_{D0}$ are regulated.

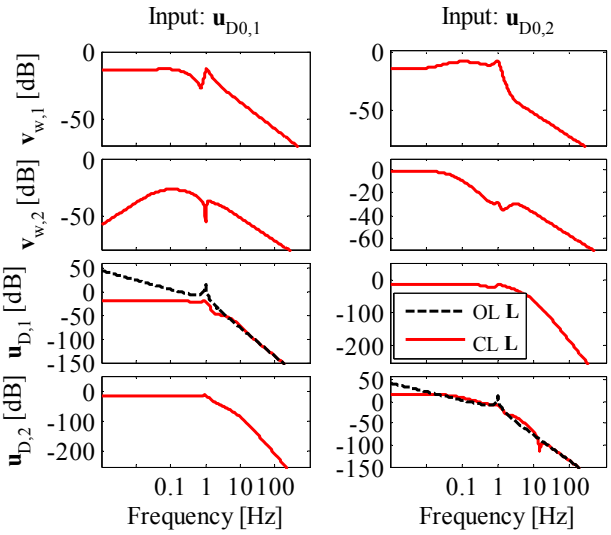

FIGURE 4: EQUIVALENT SYSTEM L IN H_∞ SYNTHESIS OF H_{FB}

The output and control inputs of the constant step disturbance (i.e. Case (a)) are shown in Fig. 5. It is noticeable that the original LQG control input $\mathbf{u}_0$ has conflicting control inputs and does not yield an energy efficient combination. Both the allocator in [16] and the proposed proxy-based allocation method converge to an optimal solution where the heavily penalized u_1 is avoided. Notice that, compared to the allocation method proposed in [16], the proxy-based allocation method does not change the original system output while the allocator in [16] introduces large deviations from the original system output. This difference fundamentally arises from the fact that the dynamic allocation method in [16] employs statically

defined null space while the proxy-based method both defines the null space and optimally allocates control efforts in broadband. This difference is further illustrated in Case (b) with sinusoidal disturbance, whose output and control inputs are shown in Fig. 6. The heavily penalized u_1 is minimally redistributed by the allocator in [16], while it is almost fully cancelled in the proposed proxy-based allocation scheme. The three input channels of the proposed proxy-based method work synergistically and thus greatly reduce the energy cost J without altering the controlled output.

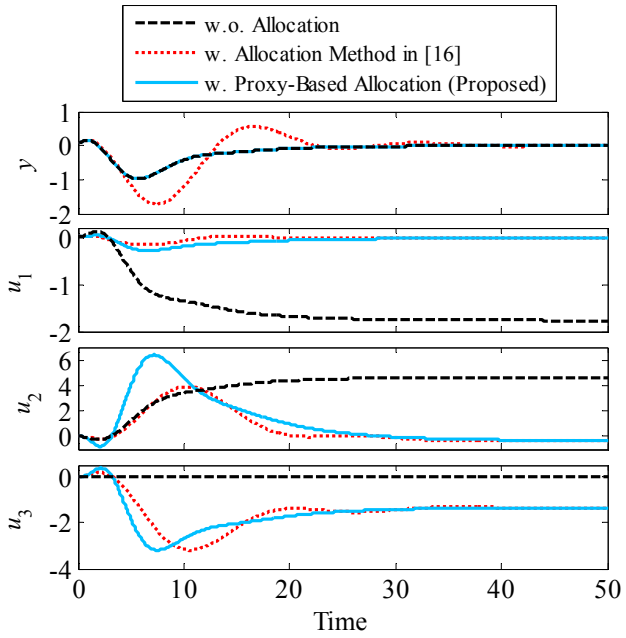

FIGURE 5: CONTROL ALLOCATION RESULTS WITH STEP DISTURBANCE (CASE (a))

To further quantify the performance of the allocators, signal $\Delta\mathbf{y}$ is defined as the output deviation from the case without allocation. Also, the steady state power consumption for each input P_1, P_2, P_3 and their combination P_{total} are defined by their contributions to the total J in unit time. $\overline{P}_{\text{total}}$ is the overall power averaged over the evaluated time horizon (i.e., including transients). The statistics for the deviations and power consumptions for Cases (a) and (b) are listed in Tab. 1. It is shown that the allocator in [16] can introduce severe output deviation, especially for the step disturbance in Case (a) where the disturbance is not continuous, while the proxy-based method's output deviations are negligible for both cases. In Case (a), both allocators consume less than 1% of the overall average power consumption of the nominal controller. Note that the overall average power consumption ($\overline{P}_{\text{total}}$) of the proposed allocator is a bit higher than that of the allocator in [16] because of the additional effort it takes to keep the output unaltered during transients; the allocator in [16] is unable to maintain the desired output during transients hence it consumes less power. However, both of the allocators converge to same static optimal control as shown in Fig. 5, resulting less than 2% steady state power difference (as observed from P_{total}). The benefit of the proposed allocator is more pronounced in Case (b), where the disturbance signal is more dynamic. The steady state power consumption of the allocator in [16] over the no allocator case is 20% less, while the proposed proxy based allocator provides 99% less steady state power consumption than the no allocator case, due to its capability to optimally redistribute dynamic control efforts (at non-zero frequencies). Note that in Case (b) the proposed allocator introduces more significant transients in some of the control efforts. This arises from the presence of NMP zeros in the controlled system, coupled with the relatively fast allocator dynamics. Even with these transients, the proposed allocator is capable of achieving 58% less overall average power consumption than the allocator in [16], based on $\overline{P}_{\text{total}}$.

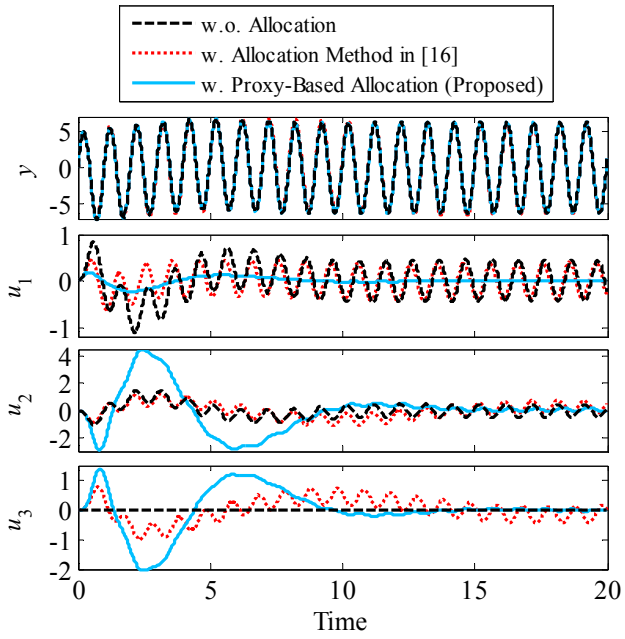

FIGURE 6: CONTROL ALLOCATION RESULTS WITH SINUSOIDAL DISTURBANCE (CASE (b))

TABLE 1: OUTPUT DEVIATION AND STEADY STATE POWER CONSUMPTION COMPARISON

		max $\lvert\Delta\mathbf{y}\rvert$	$\overline{P}_{\text{total}}$	Steady State Power			
				P_1	P_2	P_3	P_{total}
(a)	Without allocation	0	263	309	21	0	331
	Allocator in [16]	1.00	5.2	0.04	0.08	1.92	2.04
	Proposed allocator	3×10^{-5}	8.88	0.07	0.05	1.94	2.06
(b)	Without allocation	0	14.87	9.90	0.11	0	10.02
	Allocator in [16]	0.46	8.52	7.68	0.20	0.08	7.97
	Proposed allocator	1×10^{-5}	3.56	0.01	0.06	0.01	0.08

5. CONCLUSION AND FUTURE WORK

An elegant method for energy optimal control allocation for multi-input, multi-output linear time invariant over-actuated systems is proposed. Based on a quadratic energy cost, an optimal subspace is defined to describe the internal relationship of optimal control inputs. This generally non-causal optimal relationship is rearranged using matrix fraction description and spectral factorization, such that a causal and stable proxy is defined to measure the deviation from the optimal subspace. The norm of the proxy is shown to accurately measure the energy increment from optimality, and thus the control allocation problem is converted into a regulation problem, and is solved with standard H_∞ synthesis tools. The proposed proxy-based control allocation is compared with an existing dynamic allocation method in simulation studies. Significant improvements in energy efficiency without affecting system outputs are observed, especially under the influence of dynamic disturbances (at non-zero frequencies). Issues of transient shaping, constraints handling, nonlinear extensions and robustness will be discussed in future works.

ACKNOWLEDGEMENTS

This work is funded by the National Science Foundation's CAREER Award #1350202: Dynamically Adaptive Feed Drives for Smart and Sustainable Manufacturing.

REFERENCES

[1] Schneiders, M. G. E., Molengraft, M. J. G. Van De, and Steinbuch, M., 2004, "Benefits of over-actuation in motion systems," Proc. 2004 Am. Control Conf., **1**, pp. 505–510.

[2] Zheng, J., Su, W., and Fu, M., 2010, "Dual-Stage Actuator Control Design Using a Doubly Coprime Factorization Approach," IEEE/ASME Trans. Mechatronics, **15**(3), pp. 339–348.

[3] Ronde, M. J. C., Schneiders, M. G. E., Kikken, E. J. G. J., van de Molengraft, M. J. G., and Steinbuch, M., 2014, "Model-based spatial feedforward for over-actuated motion systems," Mechatronics, **24**(4), pp. 307–317.

[4] Servidia, P. A., and Pena, R. S., 2005, "Spacecraft thruster control allocation problems," IEEE Trans. Automat. Contr., **50**(2), pp. 245–249.

[5] Chen, Y., and Wang, J., 2014, "Adaptive energy-efficient control allocation for planar motion control of over-actuated electric ground vehicles," IEEE Trans. Control Syst. Technol., **22**(4), pp. 1362–1373.

[6] Tagesson, K., Sundstrom, P., Laine, L., and Dela, N., 2009, "Real-time performance of control allocation for actuator coordination in heavy vehicles," 2009 IEEE Intelligent Vehicles Symposium, IEEE, pp. 685–690.

[7] Brinkerhoff, R., and Devasia, S., 2000, "Output tracking for actuator deficient/redundant systems: multiple piezoactuator example," J. Guid. Control. Dyn., **23**(2), pp. 370–373.

[8] Halevi, Y., Carpanzano, E., and Montalbano, G., 2014, "Minimum energy control of redundant linear manipulators," J. Dyn. Syst. Meas. Control, **136**(5), p. 51016.

[9] Cheng, H., Yiu, Y.-K., and Li, Z., 2003, "Dynamics and control of redundantly actuated parallel manipulators," IEEE/ASME Trans. Mechatronics, **8**(4), pp. 483–491.

[10] Okwudire, C., and Rodgers, J., 2013, "Design and control of a novel hybrid feed drive for high performance and energy efficient machining," CIRP Ann. - Manuf. Technol., **62**(1), pp. 391–394.

[11] Johansen, T. A., and Fossen, T. I., 2013, "Control allocation—a survey," Automatica, **49**(5), pp. 1087–1103.

[12] Härkegård, O., and Glad, S. T., 2005, "Resolving actuator redundancy—optimal control vs. control allocation," Automatica, **41**(1), pp. 137–144.

[13] Härkegård, O., 2004, "Dynamic control allocation using constrained quadratic programming," J. Guid. Control. Dyn., **27**(6), pp. 1028–1034.

[14] Bodson, M., 2002, "Evaluation of optimization methods for control allocation," J. Guid. Control. Dyn., **25**(4), pp. 703–711.

[15] Petersen, J. A. M., and Bodson, M., 2006, "Constrained quadratic programming techniques for control allocation," IEEE Trans. Control Syst. Technol., **14**(1), pp. 91–98.

[16] Zaccarian, L., 2009, "Dynamic allocation for input redundant control systems," Automatica, **45**(6), pp. 1431–1438.

[17] Zhou, J., Canova, M., and Serrani, A., 2016, "Predictive inverse model allocation for constrained over-actuated linear systems," Automatica, **67**, pp. 267–276.

[18] Galeani, S., Serrani, A., Varano, G., and Zaccarian, L., 2015, "On input allocation-based regulation for linear over-actuated systems," Automatica, **52**(2015), pp. 346–354.

[19] Duan, M., and Okwudire, C. E., 2016, "Energy-efficient controller design for a redundantly actuated hybrid feed drive with application to machining," IEEE/ASME Trans. Mechatronics, **21**(4), pp. 1822–1834.

[20] Duan, M., and Okwudire, C. E., 2016, "Correction to 'Energy-efficient controller design for a redundantly-actuated hybrid feed drive with application to machining,'" IEEE/ASME Trans. Mechatronics, **21**(6), pp. 2999–3000.

[21] Duan, M., and Okwudire, C. E., 2016, "Near energy optimal control allocation for dual-input over-actuated systems," Proceedings of the ASME 2016 Dynamic Systems and Control Conference, Minneapolis, p. V001T01A011.

[22] Duan, M., and Okwudire, C. E., "Proxy-Based Energy Optimal Dynamic Control Allocation for Dual-Input, Single-Output Over-Actuated Systems," Submitt. to IEEE/ASME Trans. Mechatronics.

[23] Komzsik, L., 2014, Applied Calculus of Variations for Engineers, CRC Press.
[24] Beard, R. W., 2002, "Linear Operator Equations with Applications in Control and Signal Processing," IEEE Control Syst. Mag., **22**(2), pp. 69–79.
[25] Kailath, T., 1980, Linear systems, Prentice-Hall Englewood Cliffs, NJ.
[26] Curtain, R. F., and Zwart, H., 2012, An Introduction to Infinite-Dimensional Linear Systems Theory, Springer Science & Business Media.
[27] Sebek, M., 2015, "Spectral Factorization," Encyclopedia of Systems and Control, Springer London, London, pp. 1289–1295.
[28] Doyle, J. C., Glover, K., Khargonekar, P. P., and Francis, B. A., 1989, "State-space solutions to standard H2 and H∞ control problems," IEEE Trans. Automat. Contr., **34**(8), pp. 831–847.
[29] Francis, B. A., and Wonham, W. M., 1976, "The Internal Model Principle of Control Theory," Automatica, **12**(5), pp. 457–465.